Study design for human acuity in symbol recognition

Oliver Veitl

Bayrische Motoren Werke AG
Institute for Anthropomatics
Karlsruhe Institute of Technology (KIT), Germany
oliver.ov.veitl@bmw.de

Abstract

To date, there are no adequate quality parameters for see-through displays based on augmented and virtual reality especially for future automotive applications available. Recent approaches define detected stimuli in sinusoidal grids by their size, spatial and temporal frequency contrast sensitivity, luminance and eccentricity. The approach in this work is to know the background luminance and the display luminance distribution in order to define the contrast local rather than global for displays. This approach is based on the assumption that the ambient luminance distribution has a major influence on human visual acuity and its parameters. Therefore, a quantitative study concept is proposed based on a case study and the derivation of the relevant parameters.

By means of the described investigations it is possible to define the operating range of the optical human-machine interaction and the relevant optical parameters in head-up displays.

1   Introduction

One of the most volatile research topics of the last decade has been head-mounted and head-up displays. These displays provide additional information to the user via their visual stimulus. Acceptance of a new system depends on the quality delivered. The term quality is defined by the International Standards Organisation, short ISO, as the ability of a delivered product to satisfy all desirable and undesirable stakeholders. The relevant effects in head-up displays are optical defects.
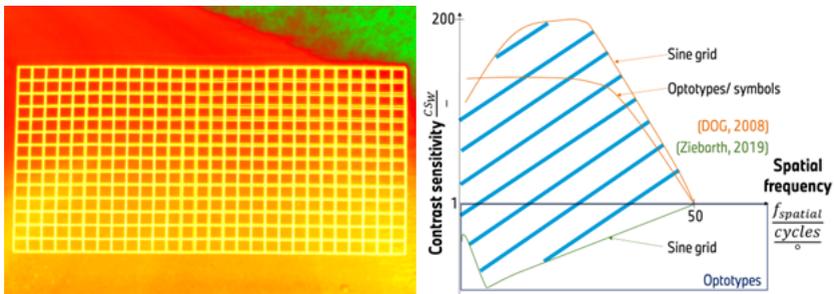

Figure 1.1: left: Luminance distribution perceived by the user of a head-up display.; right: Known fields of recognizable effects in various surroundings, see [3], [19]

Two of such effects are shown in the left part of Figure 1.1, there one can see the defined optical defects distortions and ghost images. Later can be recognized in several doubled lines in the upper right corner. It is defined as the second image detected in the direct vicinity of the first image. The order of the two images is defined by the perceived luminance difference between them, the first one is brighter than the second one. The mentioned optical distortions are defined as a deviation from an expected line. Which can be observed in the middle of the top line. The distortion can be identified at the point of the local ghost image within the run of the line from left to right.

These effects can be seen at several points in the left part of Figure 1.1. We can now ask, what kind of defects in optotypes or symbols can the human visual system detect when interacting with head-up displays? To answer this question,

it is necessary to test human visual acuity in a generalised psychophysical study. In this paper we present a possible study structure for human visual interaction with high-luminance displays.

The meaning can be derived from the right part of Figure 1.1, which shows the relation between the perceived effect and the user's environment. The environment as the contrast sensitivity ordinate is applied over the recognized spatial frequency as the abscissa. The studies carried out show a clear difference between the recognition of sinusoidal patterns and symbols within the same environment. Different environments are investigated for the recognition of sinusoidal patterns. In addition, the influence of different viewing distances in different environments is an unknown parameter. This explains the white spot of the knowledge for this research. In order to investigate the influence of adaptation and accommodation effects on symbol recognition in human vision in the context of user interaction with high luminance displays, a generalised study structure is required with respect to the relevant parameters.

In order to bring the reader up to speed, the relevant literature research results are presented in Section 2. This is followed by the preliminary remarks in Section 3 to understand our proposal in Section 4. The paper concludes with a discussion of our findings and future work.

2 Related Work

As seen in the right part of Figure 1.1, during the decade of 2010, several studies have been conducted on human pattern recognition, see [3], [19]. Der Ophthalmologe published two studies showing the difference between optotypes and sinusoidal gratings. To obtain this data, the researcher used a standardised measurement system that allows a correlation to be made between contrast sensitivity, human visual acuity and recognisable sine grids or optotypes in different environments, see [3]. The background luminance is constant during the variation of the stimulus luminance. The values and structure of the study are based on standardised procedures [11]. In parallel, a research team from Cambridge is investigating sine grating detection and possible quantification parameters with their virtual model of the human visual system, see [13]. The model consists of the comparison of two different images. The image is manipulated using parameters and formulas developed from a number of different empirical studies. A recognised image has known defects and the effects of the human visual system are added, such as neural noise and magnification functions. The latest results of this research group show a lack of knowledge in several areas. Firstly, the model is generated by different studies with different objectives, [13]; [14], secondly there are unknown parameters such as sufficient accommodation of the human eye, see [8]. The studies shown all focus on optical distortions.

These results show a scientific need for a new data set. This should include the adaptation and accommodation variance for high and low luminance displays. In addition, to fill the gap in Figure 2.1, studies should focus on optotypes and symbols. To close the gap between the studies we have shown so far and the topic of head-up displays, we will look at the other side of the recent findings.

The first study to take into account the aberrations of the mirror surface was carried out by Neumann. He discusses different optical distortions by grouping them into local and global distortions. The difference between these groups is the area of effect. This means that a global effect is seen on the entire image, as in Figure 1.1. A local effect covers a much smaller area in relation to the global effect, the difference will be clarified in Section 3, see [16]. With regard to the findings of the research team from the University of Cambridge, another

hypothesis can be made. The local distortions are optical waves with a high spatial frequency, while the global distortions have a low spatial frequency. Considering the influence of the mirror surface on the reflected image, one of the summary statements in Neumann's paper, the link to Ziebarth's research becomes clearer.

The main results of this work show the correlation between the detection of an optical defect in sinusoidal gratings and its cause. The mathematical definition of the detectable optical distortions by the contrast sensitivity function is a suitable method, as described in the previous sections. To find the cause of the distortion, the specular flux is calculated for two different frames. The conclusions show the mathematical correlation between the optical spatial frequency and the geometrical spatial frequency, see [19]. In a parallel research work, the researcher investigated the quantification of optical distortions based on convex transparent specular surfaces. In addition to the previously presented work, recognisable parameters were defined. The study examines optotypes such as the grid shown in right part of Figure 2.1. The parameters symmetry, local distortion and shape can be identified by all subjects. The deflectometric measurements of the evaluated specimens are analysed in terms of their geometric properties. Based on this knowledge, virtual specimens are calculated and additionally evaluated by the same subjects. No correlation between geometry and optical distortion was found. Two assumptions could explain the results. Firstly, the ghosted fringe patterns, sinusodial grids reflected on transparent specular surfaces, do indeed have a relevant influence on the geometric distortions. Secondly, the design of the study needs to be much more specific to the hypotheses tested, see [2]. Another study concept is to test some quantification criteria towards the human visual system. The hypothesis is not confirmed during the analysis, see [18]. All three studies on reflected image quality have one parameter in common, an assumed constant lighting scenario and therefore a constant contrast sensitivity of the subjects. Aprojanz and Wagner do not take contrast sensitivity into account. While the latter focuses on the optically evaluated optotypes and defines a contrast ratio in a non-standardised form of $90 \cdot L_{Max}/L_{Min}$, [18] the former can describe the shape deformations based on the optical distortion of the optotypes, see [2]. Comparing Ziebarth and Wagner, the dynamic evaluation of the subject makes more defects visible, see [19]; [18].

As Mantiuk et al. show the relevant influence of contrast sensitivity and the unknown influence of accommodation, [15], [8] we propose a vision system and a study structure for the evaluation of sine grids center Figure 2.1, optotype grids left Figure 2.1 and symbols right Figure 2.1, taking into account the relevant parameters.
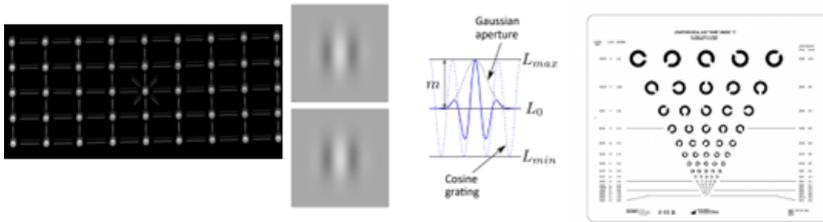

Figure 2.1: left: Tested optotype grids for head-up display quality, see [16].; center: Tested sine grids for perception values of contrast-sensitivity, see [14].; right: Tested optotype grids for precepted values of contrast sensitivity, see [17].

3 Psychophysical Relations

To understand the difference between the previous work and our new approach, in the following section we derive the model of human visual adaptation and accommodation for a high-luminance display. As can be seen in Figure 1.1, the user of such displays sees a specific image superimposed on the environment. This means that we claim that the human visual system is adapted to a certain environment, as seen in right Figure 3.1. After the superimposition, the eye accommodates to a given image, as seen in left Figure 3.1. Both of the following images are logarithmically scaled to give an idea of the actual predicted lighting scenario. We show a sunny and clear day scenario, taken with a calibrated luminance meter and a resolution of $2448 \times 2048 \cdot [Pixel \times Pixel]$.
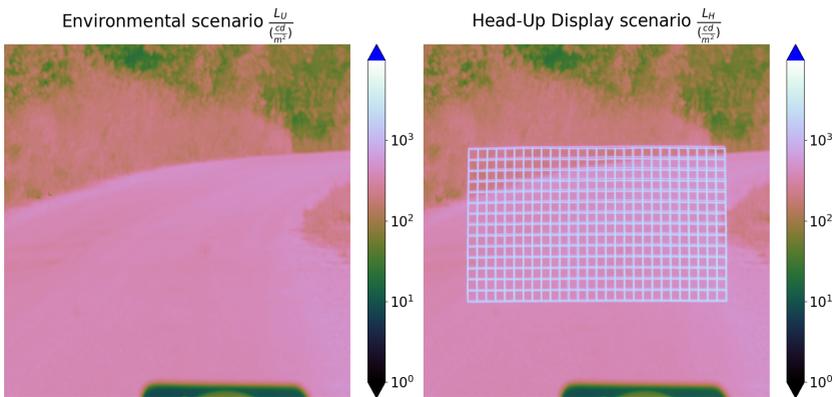

Figure 3.1: left: Adaption relevant luminance distribution.; right: Superimposed luminance distribution with accommodation relevant image.

As can be seen in the step between left Figure 3.1 and right Figure 3.1, the adaptation is independent of the superposition of the environment. This claim is based on subjective perception. If the additional luminance is influencing adaptation, the environment would become darker relative to the display luminance. Several subjective experiments have shown the same effect, i.e. the superposition of different luminance values does not affect the perceived environment.

The results in Section 2 assess this effect on the basis of the Michelson contrast. It is defined by the fraction of a luminance difference over the luminance superposition, as seen in Equation (3.1), see [14], [4].

$$C_M = \frac{\Delta L}{L} = \frac{(L_{max} - L_{min})}{(L_{max} + L_{min})} \tag{3.1}$$

The interpretation of the declarations in Equation (3.1), see [4], is shown in Figure 3.1. As we know from Section 2, since the results of Der Ophthalmologe, the contrast and contrast sensitivity in optotypes should be described by the Weber contrast function Equation (3.2), see [4]:

$$C_W = \frac{\Delta L}{L_{Max}} = \frac{(L_{max} - L_{min})}{L_{max}} \tag{3.2}$$

In this paper the put values are interpreted differently. The maximum value L_{Max} is the luminance at one point within the superimposed image, which we define as follows $[L_{HUD}] = \frac{cd}{m^2}$. The minimum value L_{min} is the measured value of the environmental luminance at the same point, defined as $[L_{Env}] = \frac{cd}{m^2}$, see [5]. Since the publication from Der Ophthalmologe the correlation between the visual acuity and the contrast sensitivity Equation (3.3) is known, see [5]:

$$CS_W = \log_{10}(\frac{1}{C_i}) = \log_{10}(\frac{1}{C_W}) \tag{3.3}$$

Contrast sensitivity in equation (3.3) is defined as $CS_W = [\frac{1}{\%}]$. This function is an essential value to describe the irradiance differences between two stimuli on the human retina. The interpretation of whether a human can recognise two stimuli or one stimulus is defined by the Rayleigh or Sparrow criteria. The application in Figure 3.1 illustrates this. The criteria are defined on the basis of the prescribed wavelength of the light and the aperture, in our case the human iris, of the maximum visual acuity, see [9]. Summarized, this means, are two lines differentiable or not. Figure 3.2 shows the computation of the human visual potential for different wavelengths based on different apertures.

The Figure 3.2 shows the computation angular visual acuity for photopic or day vision and scotopic or night vision. To describe these two scenarios, the pupil
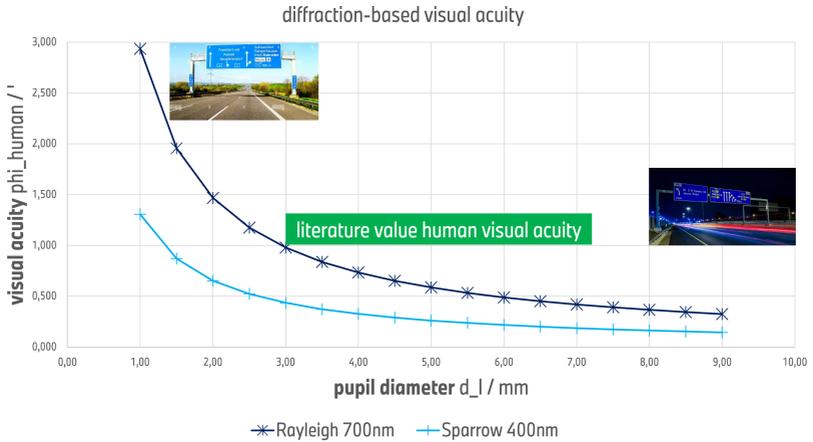
Figure 3.2: Computation of the human visual acuity in dependency of the pupil diameter for the Rayleigh criteria and the Sparrow criteria.

diameter based on the literature is used. The computation shows a possible set of solutions from $0, 86 \cdot mrad > \varphi_{Human}(1, 0 \cdot mm) > 0, 38 \cdot mrad$ down to $0, 10 \cdot mrad > \varphi_{Human}(9, 0 \cdot mm) > 0, 04 \cdot mrad$, the conversion from arc minute to radians is calculated by the constant $K_{mrad} = \frac{\pi}{(60 \cdot 180 \cdot 1.000)} \cdot \frac{mrad}{\prime}$. In comparison, the literature states the maximum visual acuity is defined as $\varphi_{Max}(Human) = 0, 29 \cdot mrad$, see [10]. This angle is defined as a function of the nodal point position and the statistical distribution of the retinal cones. Therefore, a study design needs to consider the set of solutions and the environmental parameters are elaborated.

3.1 Human vision

Since the function of the human visual system is not trivial and the psychological parameters in perception are not negligible, one should first clarify the observed parameters. The parameters and the method of observation have an additional influence on the classification of the subject study. The upper and lower Figures 3.3 show two functions. The upper in Figure 3.3 is an abstraction of an ideal adaptation scenario. It is ideal because the optical imaging of the object onto the curved image plane is free of distortion and every average ray passes through the nodal point K_i'.
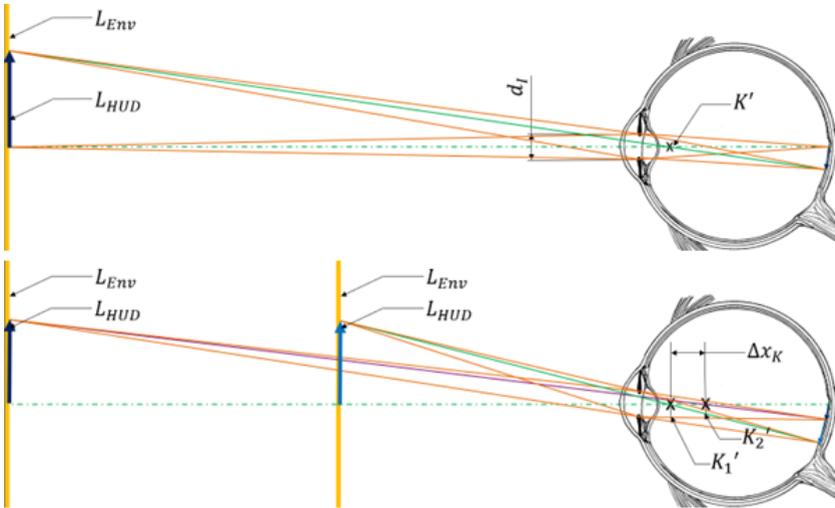

Figure 3.3: upper: Human vision adaption model for high luminance displays.; lower: Human vision accommodation model for high luminance displays.

Figure 3.3 shows the assumed adaptation model used for the study design. The human eye on the right side is based on the Gullstrand model see [4]. Its fixation point is a part of the object plane described by the luminance L_{HUD} and its orientation by the dark vector. The focused plane is surrounded by the yellow environment described by L_{Env}. Accommodation is a change in the iris diameter to limit the incoming light flux and is defined as $[d_i] = mm$. The accommodation model is abstracted in lower Figure 3.3. The Gullstrand eye model focuses on two different levels. The first is defined by the black vector starting from the optical axis and the second by the blue vector. The constant adaptation is achieved by an equal environment L_{Env}. The orientation defined by the vector and the size of the observed dark and blue image are radiated by an equal luminance L_{HUD}. An image of the same size is perceived as larger if the distance between the nodal point and the focal plane is smaller. In addition, the human eye can adjust the pupil to obtain a sharp image. A possible explanation is a longitudinal shift of the nodal point. The shift is then realised by the relaxation or contraction of the pupil. This effect results in different nodal points, K'_1 for the near image and K'_2 for the far image. In summary, the proposed study is based on the change in visual acuity, defined as $[\Delta\varphi_{Human}] = mrad$, by a variance in the adaptation-based pupil diameter d_I and the accommodation-based longitudinal nodal shift $[\Delta x_{longitudinal}] = mm$. A user may perceive different types of optical defects in the scenario shown in right Figure 3.1, distortions see left Figure 3.4, ghost images see center Figure 3.4 and disparities see right Figure 3.4.
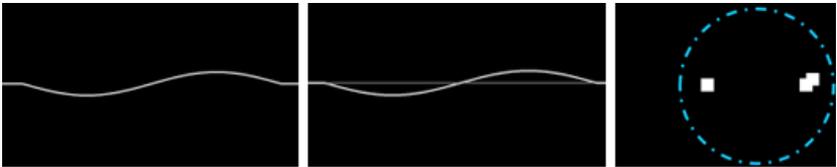

Figure 3.4: left: Distortion based on a cosine; center: Ghost image based on a cosine distortion; right: Disparitiy point shift

The distortions can be described by a wave. The mathematical definition of the functions shown is not relevant as it is only intended to clarify possible parameters. It becomes clear that amplitude, spatial frequency, contrast and

the experience of the observer influence the detection of distortions. This will be discussed in the following section. The ghost image is also influenced by the Rayleigh or Sparrow criteria already mentioned. The most complex are the disparities. Disparities are optical defects that affect the human stereoscopic vision system. Figure 3.4 (right) contains a blue circle to define the area under investigation. The area describes the spatial region in which the empirical horopter can be abstracted as a plane. The horopter is a virtual ellipse in the human environment, it describes points of equal depth estimation based on the triangulation of both eyes and the human image processing calculated by our brain. The two points are equally distant from the central plane of both eyes. On the right, there are two white shifted dots. This shift means that the points do not represent the matching cones of the right and left retinas. A new set of parameters is therefore relevant for human recognition, consisting of anthropometric data, in particular the interocular distance, and the Rayleigh or Sparrow criteria. To summarise the basics of human vision, the following parameters are considered.

$$\varphi_{Distortion} = f(d_I, x_K, \omega_{Distortion}, A_{Distortion}, CS_{W_i}) \quad (3.4)$$

$$\varphi_{Ghost} = f(d_I, x_K, \omega_{Ghost}, A_{Ghost}, CS_{W_i}) \quad (3.5)$$

$$\varphi_{Disparitiy} = f(d_I, x_K, \Delta x_{Disparity}, \Delta y_{Disparity}, CS_{W_i}) \quad (3.6)$$

Equation (3.4) describes the visual acuity $\varphi_{Distorion}$ for distortion detection in optotypes, it is a function defined by iris diameter d_I, nodal point position d_K, the spatial frequency $\omega_{Distorion}$, the defect size $A_{Distorion}$ and the contrast sensitivity CS_{W_i} between the environment and the image plane. While the detection of a ghost image depends on the same parameters, the contrast sensitivity reference additionally takes into account the irradiance of the second line in left Figure 3.4. The mathematical parameters of disparities are described by a longitudinal shift $\Delta x_{Disparity}$ and a lateral shift $\Delta y_{Disparity}$. The contrast sensitivity in the case of disparities describes the ratio between the background and the two shifted dots on the right side of right Figure 3.4. The set of new parameters needs to be considered in a single study, a properly structured study and the consideration of psychological effects, see [19]; [14].

3.2 Psychological study design

The research process of empirical investigation of psycho-physical relations follows a strict procedure. For quantitative results with high conceptual, internal, external, and statistical reliability the sequential process includes 9 steps, see [6].

1. Research topic

2. State of the art

3. Study design

4. Operationalisation

5. Sampling of subjects

6. Execution

7. Study processing

8. Analysis

9. Presentation

Steps one and two are covered in the first two sections of this paper. This chapter focuses on the third step in the upper list. In order to classify the required study, the hypotheses to be investigated are formulated at this point.

- Is there a significant difference in human visual acuity for contrast sensitivities below 1 for symbols and optotypes compared to standardised methods?

  - H_0: There is no statistically relevant difference between the concept and standardised methods.

  - H_1: The human visual acuity is statistically lower than standardized methods.

- Is there a dependence on human visual acuity for optotype defect recognition with respect to the independent variables investigated (defect size, accommodation and adaptation)?

    - H_0: No dependency function between the independent and dependent variable is found.

    - H_1: The variables dependent and independent show a relation between each other.

The hypotheses show two expected quantitative outcomes. The outcome studied or measured in psychological experiments is called the dependent variable. The varied parameters are called independent variables. Confounding variables may also influence the desired outcome. In the study design, all known variables are classified, the execution plan is structured, and the analysis method is defined taking into account the required validity, see (Döring, 2022). The validity of the study design depends on its internal and external validity and its methodological rigour. The classification of studies into the two types is helpful.

1. Research-theoretical approach

2. Knowledge objective

3. Object study

4. Data basis

5. Knowledge interests

6. Subject line-up and treatment

7. Investigation surroundings

8. Investigation repetitions (time)

9. Investigation repetitions (subject)

The desired measurement outcome influences the chosen approach by its predefined scale. If the output is unknown to the scientific community, the knowledge objective is basic research, otherwise it is called an applied research study. A study is defined by the objects studied, whether it is theoretical research in articles, methodological research for further development, or gaining new knowledge through empirical studies. This makes it possible to define the class of data needed. Is the data set generated new, so-called primary data, are there already secondary data sets that can be analysed with new methods, or is it possible to combine several existing data sets statistically for a meta-analysis? This may be done for various reasons. One reason may be an exploratory study to derive research questions or hypotheses, an explanatory study to prove pre-defined hypotheses as possible answers to open questions, or descriptive studies to test hypotheses for a representative entirety. The population to be studied is also part of the sample and its treatment. A possible subject line-up affects the quality of the data provided. To investigate a causal relation, it is recommended to choose an experimental study with randomised groups. There is no control on the group composition, but the effect can be measured by the installation of a control group. The control group is an instrument to elaborate cause and effect by variation of effect between the groups. A requirement for this installation is a parity of both groups. This method is also used in quasi-experimental studies with the difference of manipulating the group composition. Another concept that is possible are non-experimental studies. The groups are not randomized and the potential for causal investigations is low. Another important issue is the setting. Typically, designs are described as a field or laboratory study. The latter is a simulation of a real situation, while the former is measured in a real situation. The difference between these two approaches is the controllability of the confounding variables. This is where internal and external validity become more important. Both define the quality of the study results. An internally valid result provides a clear causal relation between the dependent variable and the independent variable studied. Therefore, methods such as randomisation for subject confounding and constant environmental confounding with proper control and documentation are used. Externally, a dependent variable is valid if the design and the whole are generalisable. This can be provided by a representable group of subjects. Another possibility is to specify the subject by their ability to

understand the changes during the study. These levers allow a lower variance of the dependent variable. Replication also reduces variance and increases validity. Time-based repetitions describe the use of subjects. They take part in either a within-subject study or a between-subject design. The latter omits repetitions to save time, while the former includes a preliminary measurement to increase internal validity. Within-subject designs have additional problems, depending on the particular case. One problem may be the acquisition of expertise. This is especially the case when the subject has to perform a certain task under different conditions. The time available for the task may decrease with each attempt. The final point is the repetition of tests by increasing the number of subjects. The absence of replication means that a case study has been carried out. In scientific work it is more common to carry out group studies, see [6]. In order to find a causal relation between the dependent variable and the independent one over a representative entirety, two additional points have to be clarified, the statistical analysis method and the classification of the single measurements. One single run in a conducted psychophysical study is classified by three parameters, see [12]. The first level of description is the class, followed by the dichotomous level. The first is defined by the absence of parallel stimuli. This means that a reference element can be used by the subject. Other dichotomies used to describe an experiment are decision types, evaluation types and task types, see [12]. The decision for an answer to a question can be a forced choice or a rating on a given scale. The questions relate to the subject's evaluation, such as identifying a difference or absolute steps, or detecting errors relative to a reference versus finding the worse error in discrimination tasks, and finally the objective or subjective measurement of representations. These assessment tasks are subdivided into the measurement groups of magnitudes or dimensions, called appearance, and performance measurements, related to the subject itself, see [12]. The analysis of the individual runs and the overall study can be carried out using different statistical methods in relation to the tasks. Döring emphasises the prior knowledge required for a "correct" measurement, see [6].

3.3   Statistical distributions and tests

In the last chapter the relationship between hypotheses and questions was mentioned. To test hypotheses, statistical methods are needed. The choice of the right methods depends on the data set and the idea of the possible distribution. In this section we will look at two different distributions and the mathematics of testing them. The first is a two-sided distribution, also known as a symmetric distribution, and the second is a one-sided or two-sided distribution. The latter can be described by the Chi-square method and the former by a normalisation method. Finally, a coefficient is introduced to prove a possible correlation between different variables. An example of a two-sided distribution is the normal density function. The function is symmetrical and describes the density of samples at a given value. The variance of the samples tested around a given mean or median and their density of occurrence is described by a function, see Figure 3.5. Three different distributions are shown in the figure, see [7]. The graph shows the density of the tested samples over their initial value. The dotted function has a lower variance of the output values on the abscissa and therefore a higher density of values around the mean. The dashed line, on the other hand, shows a high variance and therefore a low density of values in the range of values on the ordinate.
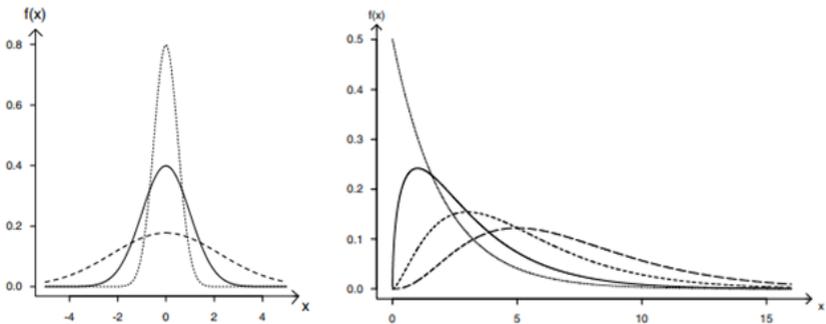

Figure 3.5: left: Normal density function, see [7].; right: Chi-squares density function, see [7].

Right Figure 3.5 shows a chi-squared density distribution for different samples tested. This function is a permutation of the normal distribution in left Figure 3.5, see [7]. The median shift is recognizable between the solid, the dashed and the dotted lines from left to right. The density of values for the specific functions shrinks in the same direction, causing the spread function to increase. A left boundary is the reciprocity of all functions in right Figure 3.5. Testing the sample distribution against a chi-square function is part of the cross-correlation tables. The reliability of the median depends on the number of samples. The ideal case is testing $N_{Samples} > 50$, a mathematical error correction is only possible for $N_{Samples} \geq 20$. Starting from the correct number of samples, it is possible to analyse a significant difference between the observed and the expected value, as shown in Equation (3.7):

$$\chi^2 = \sum_{i=1}^{k} \sum_{j=1}^{m} \frac{(h_{ij} - \tilde{h_{ij}})^2}{\tilde{h_{ij}}} \tag{3.7}$$

The test coefficient χ^2 for an $i \times j$ dimensional measurement matrix is computed by the squared distance function between the observed statistical frequencies h_{ij}, and the expected one $\tilde{h_{ij}}$ as a fraction over the expected statistical frequency $\tilde{h_{ij}}$ The function is used in various test procedures, independency test, distribution test, and homogeneity test.

$$df = (Ni - 1) \cdot (N_j) \tag{3.8}$$

To evaluate the significance, the degree of freedom is needed, computed by Equation (3.8). It takes into account the number of discretisation steps in the test matrix for $i \times j$. The computed value compared to the chi-square distribution table, see [7], provides the upper bound depending on the number of samples. As already mentioned, reliability is a strong evaluation method, therefore Equation (3.9), see [7] is a possible tool:

$$CramersV = \sqrt[2]{\frac{\chi^2}{\chi^2 + N_{Samples}}} \tag{3.9}$$

Cramérs rule or the contingency coefficient makes it possible to calculate the meaningfulness of the experiment, it should be bigger than $CramersV > 0,3$. Another possibility to analyse data is correlation analysis. Therefore, the samples are tested in multidimensional density rooms, as seen in Figure 3.6.
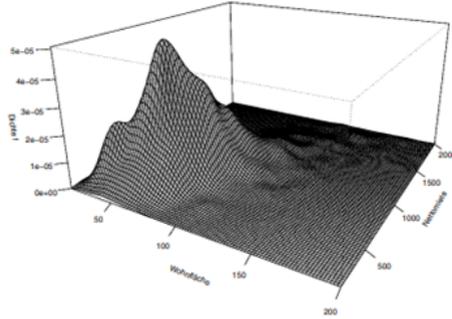

Figure 3.6: Two-dimensional density function, see [7].

The Figure 3.6 shows the density of samples over two different parameters. The computation of such a landscape is done by Bravais-Pearson (3.10) or Spearman (3.11) coefficients, see [7]:

$$r_{Pearson} = \frac{\sum_{n=1}^{k}(x_i - \bar{x}) \times (y_i - \bar{y})}{\sqrt[2]{\sum_{n=1}^{k}(x_i - \bar{x})^2 \times \sum_{n=1}^{k}(y_i - \bar{y})^2}} \qquad (3.10)$$

$$r_{Spearman} = 1 - \frac{6 \cdot \sum_{n=1}^{k}(x_{rank} - y_{rank})^2}{n_{Samples} \cdot (n_{Samples}^2 - 1)} \qquad (3.11)$$

Pearson's distribution can handle of non-linear functions, whereas Spearman's cannot. Spearman transforms the measured values of parameter one x and parameter two y of the scatterplot into a ranked list.

Whereas Pearson calculates the fraction of the summed product of the distance functions over the square root of the square sum of the individual distance functions of x and y with respect to their mean values $\bar{x}$ and $\bar{y}$. The statistical interpretation is the same for both distributions, see [7]:

$$t_i = \frac{r_i \cdot \sqrt[2]{n_S amples - 2}}{\sqrt[2]{1 - r_i^2}} \tag{3.12}$$

A significance t_i based on the distribution of Pearson p_i, equally Spearmann s_i, is given for squared values bigger $0, 1$. In the ideal case $t_i^2 > 0, 5$. Based on knowledge of statistical analysis methods, the psychophysical data acquisition and the optical conditions in the following section a study concept is derived. It considers correlation and independent variables.

4   Results

This section presents the structure of the study and the individual experiments. Relevant variables are derived from a preliminary field case study, the analysis defines boundaries and conceptual parameters. The derivation of the variable structure is based on the state of the art and the knowledge gained from the case study. Structured dependencies and variables lead to the proposed study design and experiments, taking into account the state of the art. The necessary hardware setup is then derived to investigate the variables in an environment similar to the field case.

4.1   Preliminary field case studies

This study elaborates on the variables and their limitations as mentioned in Section 3. In addition, the findings from Section 2 are taken into account in the design. During a sunny and clear day, typical user interaction scenarios are captured. Weather conditions during the night are also clear. To simulate the most accurate scenario, a tarmac road in a north-south direction is chosen. This is done to maximise the variance of the background luminance and to minimise unacceptable stray light affecting the measurement. The test is carried out on a production vehicle. Unknown parameters, see Section 3, are the adaptation-luminance relationship and accommodation. As the latter cannot be measured without violating the system under investigation, only the former is shown in Figure 4.1.
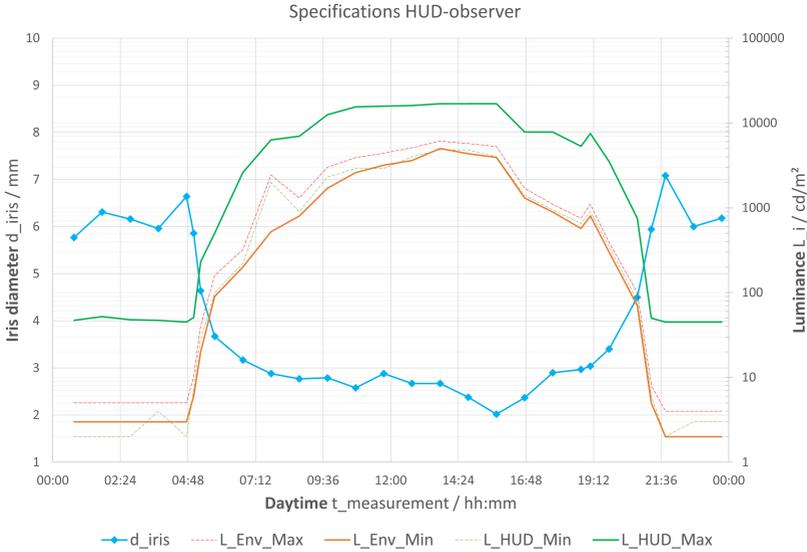
Figure 4.1: Caputered relation between the iris diameter and the lightning scenario in high-luminance displays.

The upper graph shows the specifications for human vision as defined in Section 3. Over a 24 hour period, the measured data record the diameter of a human iris on the primary ordinate and the perceived absolute luminance extremes on the secondary ordinate. The extremes are taken from the distributions shown in left Figure 3.1 and right Figure 3.1. The constant distribution at night is caused by a constant background distribution from car headlights. This results in a constant aperture diameter, taking into account the measurement uncertainty. Another effect is the adaptation of the minimum ambient luminance caused by the head-up display system. The system superimposes a grid on this distribution, as shown in right Figure 3.1. A peak in the aperture diameter is measured at sunrise and sunset. No valid explanation can be derived from the data shown. A possible hypothesis is the high level of blue light during the 'blue hour' or sunrise and the high level of red light during the 'golden hour' or dawn.

No further investigation is carried out at this point, only the maximum iris diameter during driving scenarios of $d_I = 7 \cdot mm$ is noted as a control variable. From this point on, the diameter decreases towards the base ten in the same way as the logarithmic luminance distribution. Between 8 o'clock and 18 o'clock, the diameter remains constant at a median value of $d_I = 2,7 \cdot mm$, taking into account the measurement uncertainty. The absolute minimum at 15 o'clock is disregarded due to its single occurrence and the almost constant luminance distribution over several hours, a further investigation should clarify the event. Upper boundary maxima are considered for their double appearance. Diameter-boundaries are reached at the luminance differences of $L_{Env} = 7 \cdot \frac{cd}{m^2}$ to $L_{Env} = 45 \cdot \frac{cd}{m^2}$ and $L_{HUD} = 900 \cdot \frac{cd}{m^2}$ to $L_{HUD} = 7.000 \cdot \frac{cd}{m^2}$. These situations and boarders are noted as possible boarders and need therefore another analysation towards the optical parameters mentioned in Section 3, as seen in Figure 4.2 and Figure 4.3.
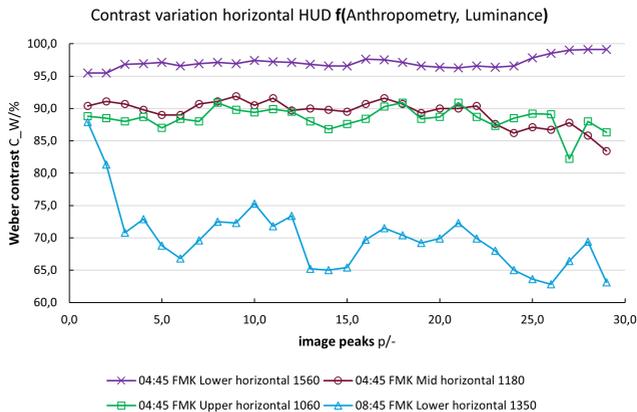

Figure 4.2: Analysation of the extremes of Figure 4.1 towards the human perceived contrast.

The discussion of Figures 4.2 and 4.3 must be done in parallel to see the relevant parameters. The ordinates show a section through the grating, see right Figure 3.1, for the calculated contrast and contrast sensitivity. Each measurement point represents a peak of the grating.

Four representative situations were chosen to define the limits. The first three data sets representing the different driver sizes are dyed in purple, green and red. The fourth one is chosen to represent a group of data sets, which are varying around a lower contrast limit of $C_W = 70 \cdot \%$. The anthropometric data, taking size into account, shows that the upper limit in terms of contrast is represented by a large driver. In terms of contrast sensitivity, which is related to human visual acuity, this is the lower limit. The upper limit is measured for the same driver at high luminance. Large internal changes in contrast distributions can be correlated with changes in background luminance.
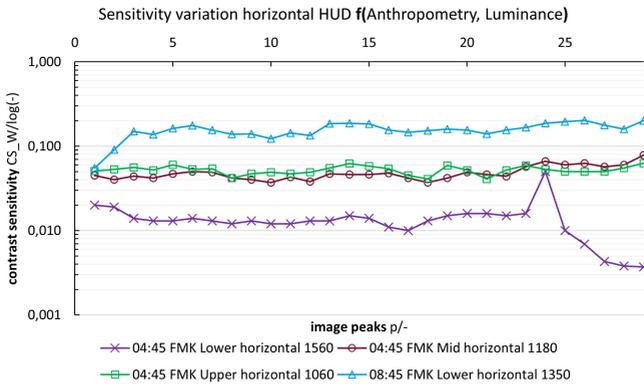

Figure 4.3: Analysation of the extremes of Figure 4.1 towards the human perceived contrast sensitivity.

The range of measurement data in Figure 4.3 proves the proposal of Section 1 towards the investigation area. Boundaries defined based on the preliminary study are $0,0037 < CS_W < 0,2$. Summarizing the knowledge of the case study and the state of the art the study structure can be set.

4.2   Psycho-physical sample study concept

In the first step, see Section 3, the relevant variables are summarized and classi-fied, see Table 4.1.

Name	Var.	Treatment	scale
Iris diameter (eye)	CV	Environment	Preliminary
Visual acuity I (eye)	IV	DIN EN ISO 8596	Preliminary
Visual acuity II (eye)	IV	Environment	Processing
Pattern orientation	DV	Horizontal/vertical	1-2
Frequency (pattern)	DV	Randomized	1-5
Amplitude (pattern)	DV	Randomized	1-5
Offset (Pattern)	DV	Randomized	1-5
Shift (Pattern)	DV	Randomized	1-5
Distance (pattern)	DV	Grouped	1-9 m
Contrast sensitivity	CV	Grouped	Preliminary

Table 4.1: Elaborated parameters from the preliminary study to be considered in the study construct.

Table 4.1 groups the relevant known parameters according to their role in the study. The independent variables, short IV, iris diameter and visual acuity, are measured during the study. These are actively manipulated by the dependent variable, short DV, and the confounding variable, short CV. As can be seen in the table, the diameter is not only a CV, but also contrast sensitivity. These variables are documented during the study to exclude singularities. Another point is the detection of fatigue symptoms by recording the diameter. Experience shows that the human visual system requires a great deal of effort to focus on high-luminance displays over time, this record makes it possible to correlate drifts within an experiment with symptoms. The third variable is measured first to falsify the first null hypothesis. The third IV is the reference visual acuity, which is measured using standardised methods, see [11]. The perceived luminance distribution is recorded to match the quantitative values in the post-processing. These values are stored for all known optical defects, see Figure 3.4. The manipulation of

horizontal or vertical lines and dots is selected in this step. As every human has a high level of experience with these optotypes, the visual system is additionally 'calibrated' to an intrinsic vertical and horizontal line, see [4]. In summary, a 3×3 study structure is required in the lighting scenarios already defined, see Figure 4.4. The study shown provides a 3×3 measurement matrix for each of the optical defects. The matrix is analysed using the correlation methods already mentioned. Each point in the matrices is obtained by a 3×5 experiment in laboratory conditions derived from the field studies described in the last chapter. As discussed in Section 2, the randomisation of stimuli and their repetition is essential for high internal validity.
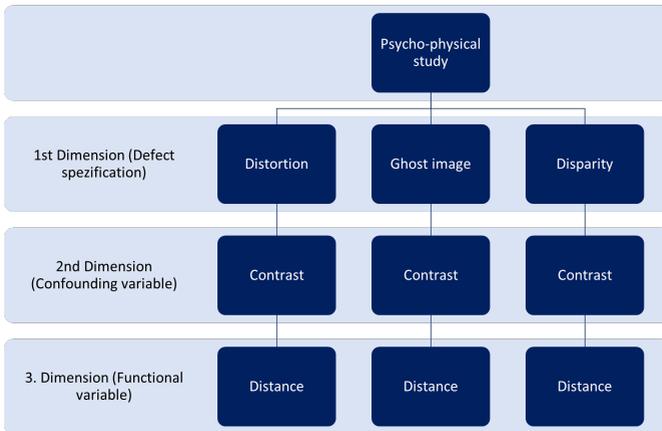

Figure 4.4: Summarized study structure for a 3×3 factor plan considering all adaption and accommodation effects.

In order to minimise the empirical and temporal effort, only the detection amplitudes for the different scenarios are divided into 5 steps. It is assumed that at least three grid points are needed to distinguish between a linear and a non-linear relation. As mentioned in Section 2, the frequency and amplitude of the defects in the patterns are decisive for the distortions. In the ghost image, the measuring points are defined by the offset between two lines and their contrast sensitivity to each other. The last type of defect is disparity, in which case two points are shifted relative to each other and their contrast sensitivity is defined, as shown

in Figure 3.1. In order to see a significant difference, the standardised acuity is measured and each value of the 3×5 contingency matrix obtained from the experiment in Figure 4.5 is analysed by the Chi-square method.
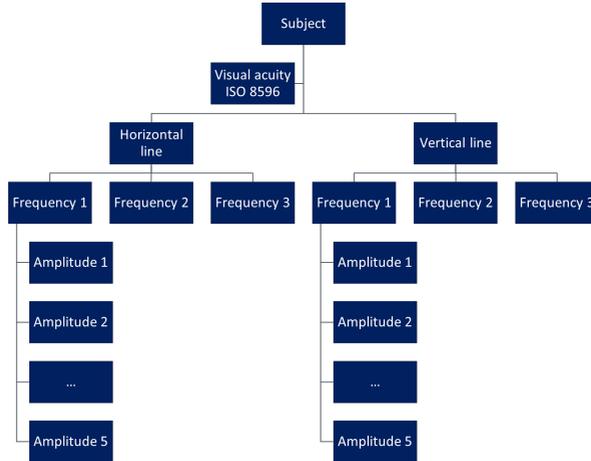

Figure 4.5: Sample experimental plan to derive the visual acuity in optotypes in comparison to standardized methods.

Before visual acuity is measured, the subject must adapt their visual system to the environment. The maximum adaptation time for photopic vision is measured as a period of ten minutes, see [1]. After the aforementioned adaptation period and acuity measurement in the final environment, full adaptation should be allowed for the forced-choice viewing of 90 images in 15 minutes.

5   Conclusion and further work

The paper presents an empirical concept based on the assumption of the importance of the local contrast sensitivity. The explanatory objectives are achieved by an optical quantitative data set derived from laboratory position experiments. The laboratory description of the parameters of the optical field study increases the external validity, whereas the internal validity is increased by the repetition of the ratings by the subject and the repetition of the experiment by different subjects. This methodology increases the statistical validity. This approach provides a complete set of primary visual acuity data. Bottle necks of the methodology can be the chosen statistical post-processing methods. Analysis of such data sets using chi-squared distributions has already been carried out, but from a critical point of view the distribution of the data is not yet known. Knowing this, we only can assume a one-sided bounded distribution, which can also be described by a log-normal distribution. The proposed optotypes also have an effect. In the case shown, lines are assumed to have a strong influence on perception. The discussion of the results is concluded by mentioning the lack of a method to control the subject's state of accommodation. A setup that fully meets the optical requirements listed in Table 4.1 is shown in Figure 5.1.
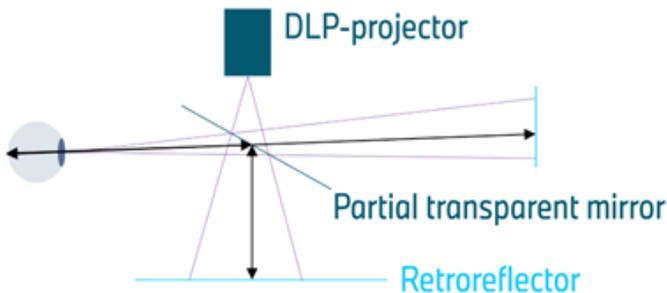

Figure 5.1: Sample experimental plan to derive the visual acuity in optotypes in comparison to standardized methods.

In Figure 5.1, the adaptation- and accommodation state can be fitted towards the research plan, see Figure 4.4, also the experimental runs, see Figure 4.5, are feasible. Further reseach will be conducted based on the already known variables, see Table 4.1. The state of the art shows the complexity for such expirements, see [8]; [14]; [19]; [3], of the human visual acuity and the obtained measurment outcome. To meet these challenges, the spatial frequencies and contrast sensitivities received by humans, as well as the theoretical perceptual amplitudes, offsets and shifts, have to be detailed. In addition, future work will propose a geometric setup that takes into account the requirements studied.

References

[1] K.R. Alexander. "Information Processing: Retinal Adaptation". en. In: *Encyclopedia of the Eye*. Elsevier, 2010, pp. 379–386. ISBN: 978-0-12-374203-2. DOI: 10.1016/B978-0-12-374203-2.00201-3. URL: https://linkinghub.elsevier.com/retrieve/pii/B9780123742032002013 (visited on 11/07/2023).

[2] Stephanie Aprojanz. *Untersuchung zur Objektivierung... durch deflektometrische Messtechnik*. de. Wiesbaden: Springer Fachmedien Wiesbaden, 2019. ISBN: 978-3-658-24369-2 978-3-658-24370-8. DOI: 10.1007/978-3-658-24370-8. URL: http://link.springer.com/10.1007/978-3-658-24370-8 (visited on 11/07/2023).

[3] M. Bach et al. "Photopisches Kontrastsehen: Örtliche Kontrastempfindlichkeit". de. In: *Ophthalmologe* 105.1 (Jan. 2008), pp. 46–59. ISSN: 0941-293X, 1433-0423. DOI: 10.1007/s00347-007-1605-y. URL: http://link.springer.com/10.1007/s00347-007-1605-y (visited on 11/07/2023).

[4] *DIN 5340*. Standard. Genf, Schweiz, 2022. DOI: 10.31030/3371845. URL: https://www.beuth.de/de/-/-/356879010 (visited on 11/07/2023).

[5] e.V. DOG. "Prüfung des Kontrast- oder Dämmerungssehens". de. In: *Ophthalmologe* 108.12 (2011), pp. 1195–1198. ISSN: 0941-293X, 1433-0423. DOI: 10.1007/s00347-011-2488-5. URL: http://link.springer.com/10.1007/s00347-011-2488-5 (visited on 11/07/2023).

[6] Nicola Döring. *Forschungsmethoden und Evaluation in den Sozial- und Humanwissenschaften*. ger. 6., vollständig überarbeitete, aktualisierte und erweiterte Auflage. Lehrbuch. Berlin [Heidelberg]: Springer, 2022. ISBN: 978-3-662-64762-2 978-3-662-64761-5. DOI: 10.1007/978-3-662-64762-2.

[7] Ludwig Fahrmeir et al. *Statistik*. Springer-Lehrbuch. Berlin, Heidelberg: Springer Berlin Heidelberg, 2016. ISBN: 978-3-662-50371-3 978-3-662-50372-0. DOI: 10.1007/978-3-662-50372-0. URL: http://link.springer.com/10.1007/978-3-662-50372-0 (visited on 11/07/2023).

[8] Dounia Hammou. "Comparison of metrics for predicting image and video quality at varying viewing distances". English. In: *IEEE MMSP* (2023). URL: https://www.cl.cam.ac.uk/~rkm38/pdfs/hamond2023_view_dist_metrics.pdf.

[9] Eugene Hecht. *Optik*. ger. Trans. by Karen Lippert. 8. Auflage. De Gruyter Studium. Berlin Boston: De Gruyter Oldenbourg, 2023. ISBN: 978-3-11-102525-4.

[10] Ekbert Hering and Rolf Martin, eds. *Optik für Ingenieure und Naturwissenschaftler: Grundlagen und Anwendungen: mit zahlreichen Bildern, Tabellen, Beispielen*. ger. München: Fachbuchverlag Leipzig im Carl Hanser Verlag, 2017. ISBN: 978-3-446-44281-8.

[11] *ISO 8596*. Standard ISO 8596. Genf, Schweiz: Beuth Verlag, 2018. DOI: 10.31030/2744962. URL: https://www.beuth.de/de/-/-/278501784 (visited on 11/07/2023).

[12] Frederick A. A. Kingdom and Nicolaas Prins. *Psychophysics: a practical introduction*. Second edition. OCLC: ocn946067924. Amsterdam: Elsevier/Academic Press, 2016. ISBN: 978-0-12-407156-8.

[13] Rafał Mantiuk et al. "HDR-VDP-2: a calibrated visual metric for visibility and quality predictions in all luminance conditions". en. In: *ACM SIGGRAPH 2011 papers*. Vancouver British Columbia Canada: ACM, July 2011, pp. 1–14. ISBN: 978-1-4503-0943-1. DOI: 10.1145/1964921.1964935. URL: https://dl.acm.org/doi/10.1145/1964921.1964935 (visited on 11/07/2023).

[14] Rafał K. Mantiuk, Maliha Ashraf, and Alexandre Chapiro. "stelaCSF: a unified model of contrast sensitivity as the function of spatio-temporal frequency, eccentricity, luminance and area". en. In: *ACM Trans. Graph.* 41.4 (July 2022), pp. 1–16. ISSN: 0730-0301, 1557-7368. DOI: 10.1145/3528223.3530115. URL: https://dl.acm.org/doi/10.1145/3528223.3530115 (visited on 11/07/2023).

[15] Rafal K. Mantiuk, Dounia Hammou, and Param Hanji. "HDR-VDP-3: A multi-metric for predicting image differences, quality and contrast distortions in high dynamic range and regular content". In: (2023). Publisher:

arXiv Version Number: 1. DOI: 10.48550/ARXIV.2304.13625. URL: https://arxiv.org/abs/2304.13625 (visited on 11/07/2023).

[16]   Alexander Neumann. "Simulationsbasierte Messtechnik zur Prüfung von Head-up Displays". Deutsch. PhD thesis. Technische Universität München, 2012. URL: https://nbn-resolving.de/urn/resolver.pl?urn:nbn:de:bvb:91-diss-20120227-1079689-1-0.

[17]   Visus. *Visustafel Landoltringe*. Nov. 2023. URL: https://www.visus.de/media/image/ab/ef/09/81685_600x600.png (visited on 11/07/2023).

[18]   Daniel Wagner. "Wahrnehmung von Augmented Reality Head-up Displays". de. In: (2023). Medium: PDF Publisher: Karlsruher Institut für Technologie (KIT). DOI: 10.5445/IR/1000154589. URL: https://publikationen.bibliothek.kit.edu/1000154589 (visited on 11/07/2023).

[19]   Mathias Ziebarth. "Wahrnehmungsgrenzen kleiner Verformungen auf spiegelnden Oberflächen". de. In: (2019). Medium: PDF Publisher: KIT Scientific Publishing. DOI: 10.5445/KSP/1000090271. URL: https://publikationen.bibliothek.kit.edu/1000090271 (visited on 11/07/2023).